Wetland Monitoring with Polarimetric SAR Change Detection Methods

A. Schmitt[a], B. Brisco[b], S. Kaya[b], A. Roth[a], A. Mueller[a]

[a]German Aerospace Center (DLR), German Remote Sensing Data Center (DFD),
Muenchner Strasse 20, 82234 Wessling, Germany – (andreas.schmitt, achim.roth, andreas.mueller)@dlr.de
[b]Canada Centre for Remote Sensing, Earth Sciences Sector, Natural Resources Canada,
588 Booth Street, Ottawa, ON, K1A0Y7, Canada – (brian.brisco, shannon.kaya) @nrcan.gc.ca

Abstract - SAR sensors have shown a high potential in surface water monitoring. Polarimetric acquisitions especially are well suited for detecting different land cover types, e.g. open water surfaces, vegetation, flooded vegetation etc. In combination with advanced change detection techniques temporal changes of land cover can be mapped covering a large area over the whole year. This paper will report on the application of a Curvelet-based change detection algorithm on full-polarimetric data acquired by the Canadian RADARSAT-2 sensor over a wetland in New Brunswick, Canada. One parameter – the alpha angle – of the Cloude-Pottier decomposition describing the type of backscatter mechanism is introduced to the Curvelet-based image enhancement and change detection method in order to extract flooded vegetation and map the changes from April to August.

Keywords: Environment, Vegetation, Ecosystem, Hydrology, Land Cover, Mapping, Floods

1. INTRODUCTION

Wetlands play a key role in the ecosystems of many countries. These huge fresh water reservoirs are able to prevent floods by holding back precipitation for a certain time as well as they can provide drinking or irrigation water even in summer time. Hence, the exploration and the protection of wetlands will be one main issue with regard to climate change. Due to the high variability of flooded areas in both space and time remote sensing techniques – especially the weather and illumination independent Synthetic Aperture Radar sensors – are essential tools for wetland monitoring. The use of SAR sensors for water resource applications has been examined in previous work (Brisco et al., 2008). A special characteristic of the active mono-static side-looking sensor concerns smooth surfaces like open water. As the incoming signal is reflected away from the sensor nearly completely these surfaces appear very dark. This fact enables the extraction of a surface water mask with automatic (Hahmann et al., 2010) and semi-automatic methods (Brisco et al., 2009). The standard single-polarized SAR image can only distinguish between high and low backscattering whereas the recent polarimetric SAR sensors are able to measure up to four different polarizations at once. These polarimetric images allow us to distinguish different scattering mechanisms in the wetlands (Brisco et al., 2011).

Freeman and Durden (1998) decompose the total backscattered intensity into the contribution of three scattering mechanisms: rough surface, double bounce and volume scattering. This approach is easy to interpret when looking at wetlands. Rough surfaces mainly can be found over grassland or dense canopy. Volume scattering is attributed to forested areas. The double bounce scattering indicates flooded vegetation where the tree trunks and the water surface form a strong reflector. The benefit of the Freeman-Durden decomposition for wetland monitoring has been examined using RADARSAT-2 data over a Canadian study site by Schmitt et al. (2010). An alternative approach reducing the scattering mechanism identification to only one layer was presented by Cloude and Pottier (1999). The so-called mean alpha angle attaches an averaged scattering event to each resolution cell by adopting values between 0° and 90°. Low values correspond to surface scattering whereas mean values indicate volume scattering and high values stand for double bounce scattering. The two other parameters – entropy and anisotropy – describe the diversity of the scattering mechanism, but these are of lower interest for wetland applications (Schmitt et al., 2010b).

Because of the high noise level of SAR data in general and polarimetric SAR data especially it is necessary to introduce novel methods to discriminate apparent structures from noise. Schmitt et al. (2009) developed a Curvelet-based approach for image enhancement and change detection in multi-temporal image acquisitions. This method can also be applied to multi-polarized data sets as shown by Schmitt et al. (2010a). The kernel of this method is the transform of the original logarithmically-scaled image to the Curvelet coefficient domain where each coefficient corresponds to the strength of a belonging linear structure in the image (Candès and Donoho, 1999). These coefficients can be weighted in order to suppress noise – assumed for low coefficients – and to preserve or enhance structures – indicated by high coefficients. After the inverse transform the image is very smooth but all apparent structures are preserved while standard filtering methods often blur fine structures or leave fine-structured areas unsmoothed. As the complex coefficient difference equals the image difference, structure-based change detection in the Curvelet coefficient domain becomes visible. The image enhancement subsequently reduces the impact of noise and results in distinct changes.

2. METHODOLOGY

The polarimetric images presented here have been acquired by the Canadian space-borne SAR sensor RADARSAT-2 in the "FineQuad" mode monthly from April to August 2010. One image product consists of four complex channels: HH, HV, VH, VV, where the letters denote the receiving and sending polarization – horizontal or vertical – of the SAR sensor. As HV and VH are the same for monostatic SAR systems like RADARSAT-2, three channels remain. The

amplitudes of the measured layers – known as lexicographic decomposition – are shown in Figs. 1-5, where the colours red, green and blue refer to the amplitudes of the HH, HV and VV channels.

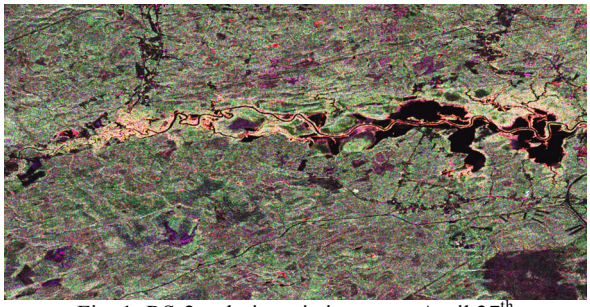

Fig. 1: RS-2 polarimetric image on April 27th

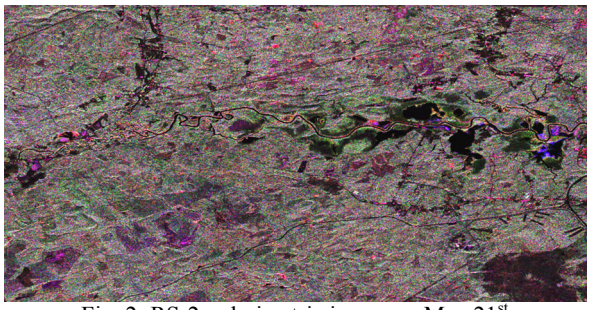

Fig. 2: RS-2 polarimetric image on May 21st

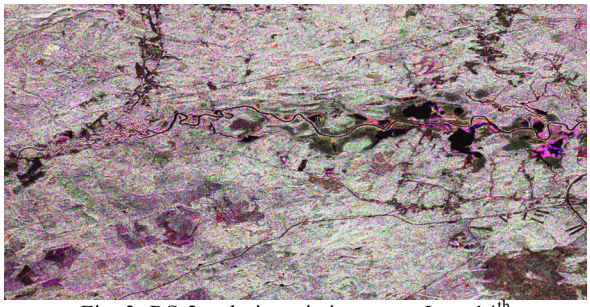

Fig. 3: RS-2 polarimetric image on June 14th

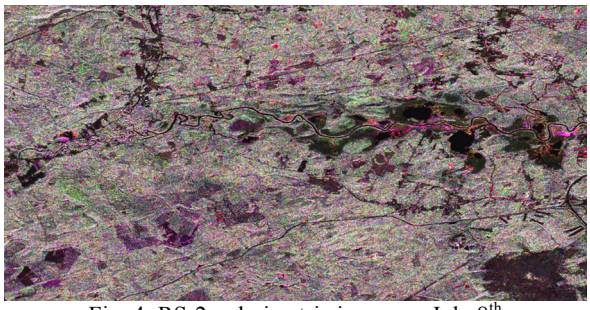

Fig. 4: RS-2 polarimetric image on July 8th

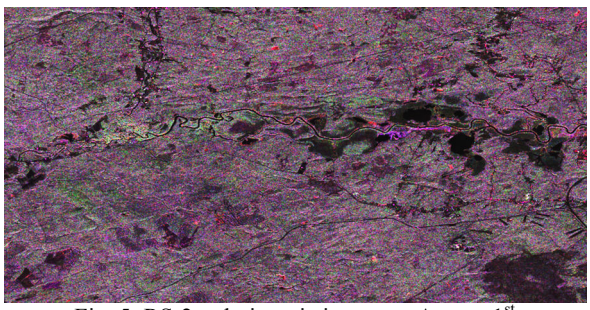

Fig. 5: RS-2 polarimetric image on August 1st

Having a look at Fig. 1 several black patches in the middle of the image can be perceived that seem to surround a thin black line. As very dark surfaces can directly be related to open water, the river and the surrounding flooded areas can easily be delineated. By comparing Fig. 1 to Figs. 2-5 one may remark that the dark regions are decreasing from spring until summer which indicates the decrease in the water gauge. Around these open water surfaces some very bright patches in Fig. 1 and some pink patches in the remaining figures respectively are visible. This might point at a double bounce effect which is always combined with a very strong backscattering intensity. To be sure of that the Cloude-Pottier decomposition is applied in order to extract the scattering mechanism. Contrary to the method described in the introduction the dominant alpha angle is chosen to represent the scattering mechanism. The Cloude-Pottier decomposition extracts three scattering events for each resolution cell. The mean alpha angle commonly used for classification purposes is the weighted average of the three alpha angles. Thus, it is a mixture of the underlying scattering mechanisms. As we always will have several scattering mechanisms mixed up over bank zones in wetlands it makes sense to concentrate on the dominant scattering mechanism - described by the dominant alpha angle – instead of the averaged one. Unfortunately the dominant alpha angle is characterized by a higher noise level than the averaged alpha angle. To compensate this drawback the Curvelet-based image enhancement is utilized.

Though developed for SAR amplitude data, the Curvelet-based image enhancement approach also works very well on layers with additive character and fixed range like the alpha angle of the Cloude-Pottier decomposition. Exactly the same coefficient weighting functions can be applied to suppress noise and to enhance structures. The results of the image enhancement step are shown in Figs. 6-10 for every image acquisition. The values of the dominant alpha angle are coded in gray scale. The mean gray symbolizes mean alpha angle and hence, volume scattering, which can be found in most of the image. Darker patches mark low alpha angle values that stand for surface scattering. Only a few isolated patches of surface scattering are shown during the time series. Very bright structures indicate a high alpha angle which means double bounce scattering. The double bounce mainly can be found around the river. These areas show a high temporal variability and a significant decrease from April to August.

In order to map the changes the difference images between two neighbouring image acquisitions have been determined by the help of the Curvelet-based change detection. The difference images hold positive and negative values as well to be able to represent an increase and a decrease in the alpha angle. In Fig. 11-14 the detected changes are illustrated. Blue tones stand for a decrease in the alpha angle of more than 10° for the pale blue and more than 30° for the dark blue. In contrast red marks an increase beginning from 10° for the orange to more than 30° for the dark red. Regions without significant changes have been made transparent so that the underlying dominant alpha angle layer – here without image enhancement – becomes visible. Obviously most changes happen between April and May. Later on, only few areas with distinct changes can be observed. However, these areas show changes over the season while the surrounding areas stay very stable except for the image acquisition of July 8th where Fig. 13 indicates a slight increase and Fig. 14 an equally slight decrease. This phenomenon presumably refers to a meteorological event that happened just before

the image acquisition, e.g. a rainfall. Wet leaves would show a different dielectric behaviour and thus, a different backscattering in the SAR image.

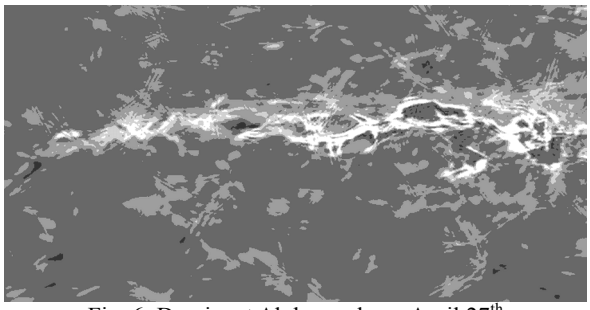

Fig. 6: Dominant Alpha angle on April 27th

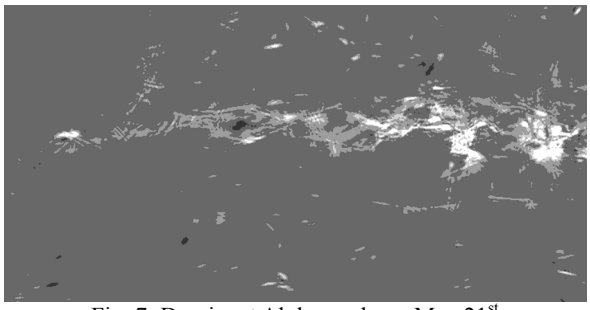

Fig. 7: Dominant Alpha angle on May 21st

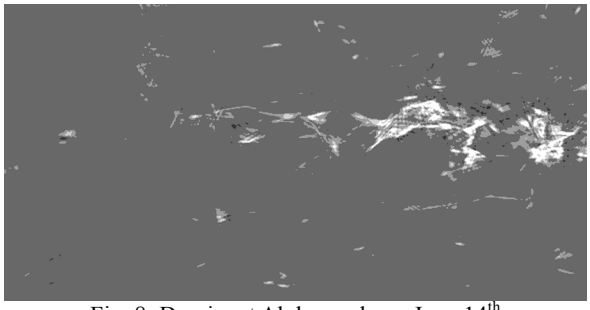

Fig. 8: Dominant Alpha angle on June 14th

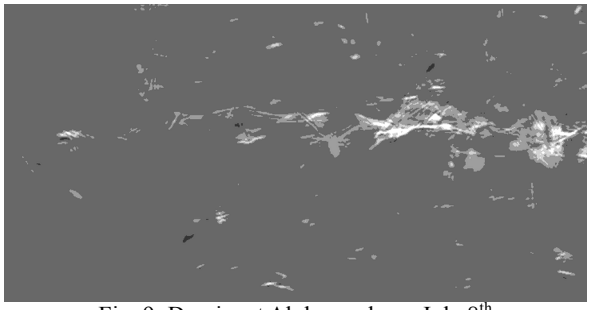

Fig. 9: Dominant Alpha angle on July 8th

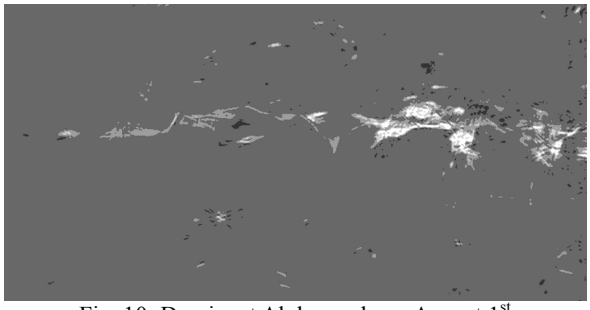

Fig. 10: Dominant Alpha angle on August 1st

3. INTERPRETATION

As aforementioned the double bounce scattering – indicated by high values of the alpha angle – can be interpreted as flooded vegetation. An increase in the alpha angle consequently indicates a change in the scattering mechanism away from a surface scatterer towards a double bounce scatterer. A decrease in the alpha angle inversely marks a move away from double bounce scattering towards surface scattering. Volume scattering is lying in-between and can be recognized as medium scattering event related to the alpha angle definition. Now, the question is how to correlate the observed change in the scattering mechanism with flooding events in the wetland.

The first difference image (Fig. 11) marks a significant decrease in double bounce scattering along the river banks. This fact is quite easy to explain: the sinking water level from April to May causes the formerly flooded forest around the river to fall dry. Larger patches mainly in the left part of the image show the same effect even though it is not that distinctive. Other regions – painted in red – mark an increase in flooded vegetation. At first glance this cannot be explained by the sinking water level. But, taking into account that flooding in spring can overwhelm shallow vegetation completely these areas correspond to vegetation that was totally covered by water and is now sticking out because of the falling water level. The comparison of the original images in Fig. 1 and 2 proves this assumption. The areas in question show an open water surface in April, but no more in May. From May on the river banks show stable backscattering.

Areas with distinct changes narrow down to some basins near the river (see Figs. 12-14). It is most remarkable that these regions do not show a steady development like it could be observed along the river banks. So, we can identify areas that fall dry from May to June and were flooded again from July to August. In the same way it is possible to delineate regions that are dry in July exclusively. As two larger patches in dark red as well as two elongate patches in orange along the river (left part of Fig. 14) indicate an increase of flooded vegetation from July to August one can conclude that the water level is raised. In order to measure the water a digital elevation model coregistered to the SAR image would be sufficient.

Evaluating the changes in the whole time series it is easy to identify different types of regions: stable regions whose backscattering mechanism does not change, regions flooded once that fall dry in spring and stay stable during summer time and regions flooded frequently. The latter indicate very flat terrain with an elevation near the mean water level so that every water level change influences the flooding situation. This might be a first step to identify different types of habitats for plants and animals. Although all observed changes can be explained logically it is necessary to validate the results. Ground truth data was gathered contemporarily to the image acquisitions and will be compared to the remote sensing results as soon as possible.

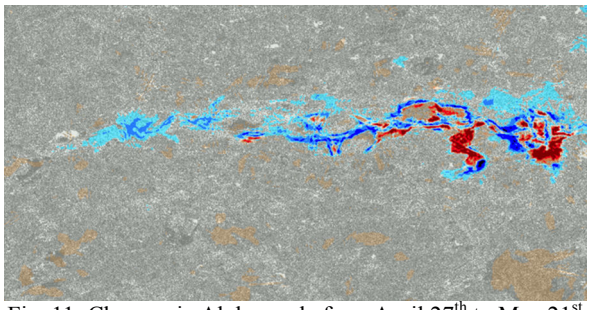

Fig. 11: Changes in Alpha angle from April 27th to May 21st

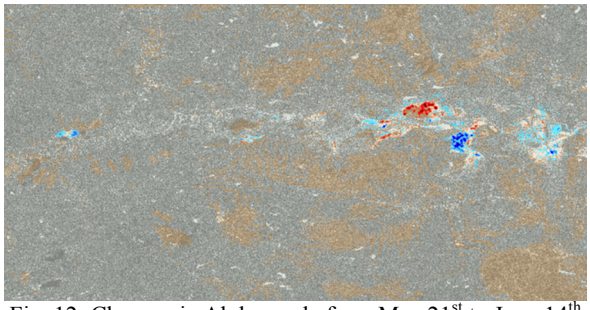

Fig. 12: Changes in Alpha angle from May 21st to June 14th

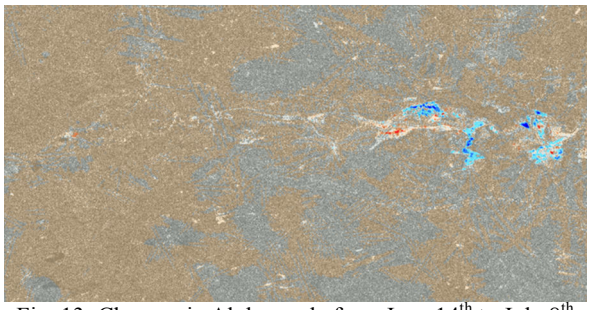

Fig. 13: Changes in Alpha angle from June 14th to July 8th

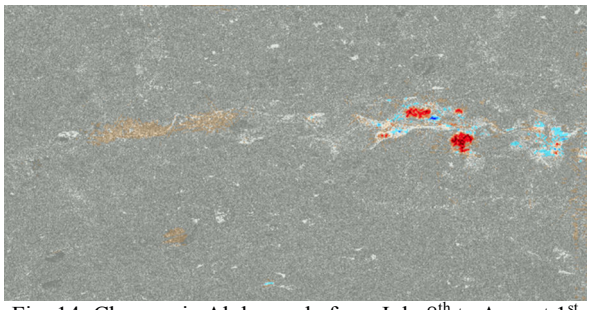

Fig. 14: Changes in Alpha angle from July 8th to August 1st

4. CONCLUSION

The combination of the Curvelet-based image enhancement and the dominant alpha parameter derived by the Cloude-Pottier decomposition of polarimetric SAR images enables the long-term monitoring of flooded vegetation in wetlands. In single images flooded areas with vegetation sticking out of the water can clearly be identified. By comparing the dominant alpha angle of images in time series the change in the backscattering mechanism can directly be related to flooding and drying events in the imaged wetland. Future work will include validation with ground truth and concentrate on the inclusion of other SAR sensors like TerraSAR-X to increase the information content and temporal coverage.

ACKNOWLEDGMENTS

This collaboration between DLR and CCRS was partially funded by the Bayern-Pfalz-Foundation in Munich (Germany) and the German Academic Exchange Service (DAAD). The Remote Sensing Science (RSS) program at CCRS also supported this research project. The authors would like to thank the above-named organizations for their financial and administrative support.

REFERENCES

B. Brisco, R. Touzi, J.J. van der Sanden, F. Charbonneau, T.J. Pultz and M. D'Iorio, "Water resource applications with RADARSAT-2 – a preview," International Journal of Digital Earth, 1(1), pp. 130-147, 2008.

B. Brisco, N. Short, J.J. van der Sanden, R. Landry and D. Raymond, "A semi-automated tool for surface water mapping with RADARSAT-1," Canadian Journal of Remote Sensing, 35(4), pp. 336-344, 2009.

B. Brisco, M. Kapfer, T. Hirose, B. Tedford and J. Liu, "Evaluation of C-band Polarization Diversity and Polarimetry for Wetland Mapping," Accepted for publication in Special Issue on SAR & Agriculture, Canadian Journal of Remote Sensing, 2011.

E.J. Candès and D.L. Donoho, "Curvelets – a surprisingly effective non-adaptive representation for objects with edges," In: Curve and Surface Fitting. Innovations in Applied Mathematics, Vanderbilt University Press, Saint-Malo (France), pp. 105-120, 1999.

S.R. Cloude and E. Pottier, "An Entropy Based Classification Scheme for Land Applications of Polarimetric SAR," IEEE Transactions on Geoscience and Remote Sensing, 35(1), pp. 68-78, 1997.

A. Freeman and S.L. Durden, "A Three-Component Scattering Model for Polarimetric SAR Data," IEEE Transactions on Geoscience and Remote Sensing, 36(3), pp. 963-973, 1998.

T. Hahmann, A. Twele, S. Martinis and M. Buchroithner, "Strategies for the Automatic Extraction of Water Bodies from TerraSAR-X / TanDEM-X data," In: Geographic Information and Cartography for Risk and Crisis Management, Towards Better Solutions. Lecture Notes in Geoinformation and Cartography. Springer-Verlag Berlin Heidelberg, pp. 129-141, 2010

A. Schmitt, B. Wessel and A. Roth, "Curvelet approach for SAR image denoising, structure enhancement, and change detection," In: U. Stilla, F. Rottensteiner and N. Paparoditis (Eds.), CMRT09, IAPRS, XXXVIII (3/W4), Paris (France), pp. 151-156, September 2009.

A. Schmitt, B. Wessel and A. Roth, "Introducing Partial Polarimetric Layers into a Curvelet-based Change Detection," In: Proceedings of EUSAR 2010, 8th European Conference on Synthetic Aperture Radar, Aachen (Germany), pp. 1018-1021, June 2010a.

A. Schmitt, B. Brisco, S. Kaya and K. Murnaghan, "Polarimetric Change Detection for Wetlands," IAHS Red Book, Centre for Ecology and Hydrology, Wallingford, Oxfordshire, OX10 8BB, UK, Remote Sensing and Hydrology Symposium, Jackson Hole, Wyoming (USA), Sept. 2010b.